Direct measurements of the spin and valley splittings in the magnetization of a Si/SiGe quantum well in tilted magnetic fields

M. A. Wilde,* M. Rhode, Ch. Heyn, D. Heitmann, and D. Grundler
Institut für Angewandte Physik, Universität Hamburg, Jungiusstrasse 11, 20355 Hamburg, Germany

U. Zeitler
HFML, Radboud University Nijmegen, Toernooiveld 7, 6525 ED Nijmegen, The Netherlands

F. Schäffler
Institut für Halbleiter- und Festkörperphysik, Johannes-Kepler-Universität Linz, Altenbergerstrasse 69, A-4040 Linz, Austria

R. J. Haug
Institut für Festkörperphysik, Universität Hannover, Appelstrasse 2, 30167 Hannover, Germany
(Received 1 July 2005; revised manuscript received 29 August 2005; published 28 October 2005)

We present de Haas–van Alphen (dHvA) measurements on high-mobility two-dimensional electron systems formed in modulation-doped Si/SiGe (100) quantum wells and demonstrate directly the manifestation of the valley splitting in the magnetization. We resolve sawtoothlike magnetization oscillations at even filling factors which reflect the Landau quantization and the spin splitting of Landau levels in the electronic energy spectrum. At odd filling factors we observe the lifting of the valley degeneracy in Si at high magnetic field. The magnetization is a thermodynamic quantity that at low temperature reflects the ground-state energy of the interacting electron system. We can thus determine quantitatively the energetic splitting of the two occupied conduction-band valleys directly from the oscillation amplitude. Both valley and spin splitting are found to be enhanced by electron-electron interactions. The energy gap due to valley splitting is found to be $\geqslant 0.8$ meV at high perpendicular field $B_\perp$. From studies in tilted magnetic fields we find that the valley splitting is governed solely by $B_\perp$. From the spin splitting we recalculate an enhanced g factor $g^*=2.9$ at $\nu=2$ including the influence of disorder. This is significantly larger than the band-structure g factor of 2 in Si. We have successfully applied the coincidence technique for the dHvA effect and thus obtained a complementary means to determine the g factor. It yields a constant value $g^* \cong 3.2$ for filling factors $\nu \geqslant 10$. A detailed analysis of the magnetization traces enabled us also to determine quantitatively the residual level broadening Γ in this high-mobility Si/SiGe system. We obtain a small value of $\Gamma = 0.15\ \text{meV} \times B_\perp\ [\text{T}]^{1/2}$ for the Si/SiGe heterostructure of 200 000 $\text{cm}^2/(\text{V s})$ mobility at 0.3 K.

DOI: 10.1103/PhysRevB.72.165429 PACS number(s): 73.43.Fj, 73.20.At, 73.21.Fg

I. INTRODUCTION

In the early days of two-dimensional electron systems (2DES's), Si metal-oxide-semiconductor field-effect transistors (MOSFET's) played a central role in basic research, culminating in the discovery of the quantum Hall effect in 1980.[1] In the 1980s most attention in basic research shifted towards GaAs heterostructures owing to the much higher mobilities achieved. With the advent of modulation-doped Si/SiGe heterostructures, mobilities in the Si system became an order of magnitude larger than in silicon MOSFET's. This opens the unique possibility to study the effects of the spin and valley splitting of the Landau levels (LL's) in silicon in much more detail than before. Especially the valley splitting and the much higher ratio of Zeeman and cyclotron energy, $E_Z/\hbar\omega_c$ (with the cyclotron frequency $\omega_c = eB/m^*$), in comparison to GaAs make Si/SiGe heterostructures a very interesting system for basic research. The former makes Si effectively a double-layer electron system with strong interlayer interactions,[2] while the latter offers the opportunity to investigate the mechanism of the spin splitting in more detail.[3] Both splittings are expected to be strongly influenced by many-body interactions, since, in experimentally accessible fields B, the Coulomb energy $E_C = e^2/4\pi\epsilon\epsilon_0 l_B$ (with the magnetic length $l_B = \sqrt{\hbar/eB}$) exceeds $\hbar\omega_c$ significantly. The important role of electron-electron interactions in conjunction with the valley splitting in the Si/SiGe system was highlighted recently by Lai *et al.*,[4] who investigated the fractional quantum Hall effect in Si/SiGe by means of magnetotransport. The results could be quantitatively interpreted in a picture of composite fermions with the valley degree of freedom. Until present, the highly complex energy-level structure in Si-based 2DES's was mainly addressed by means of transport experiments.[5–9]

In this paper we report on low-temperature studies of the magnetization of 2DES's in Si/SiGe (100). The magnetization is a thermodynamic quantity defined by $M = -(\partial F/\partial B)|_{N,T}$, with the free energy F, and is thus particularly suited to investigate the electronic ground-state properties and the density of states (DOS) of 2DES's. Measurement of M thus provides important new information about the spin and valley splitting in Si/SiGe as compared to traditional transport experiments. We observe a sawtoothlike de Haas–van Alphen (dHvA) effect at even filling factors ν

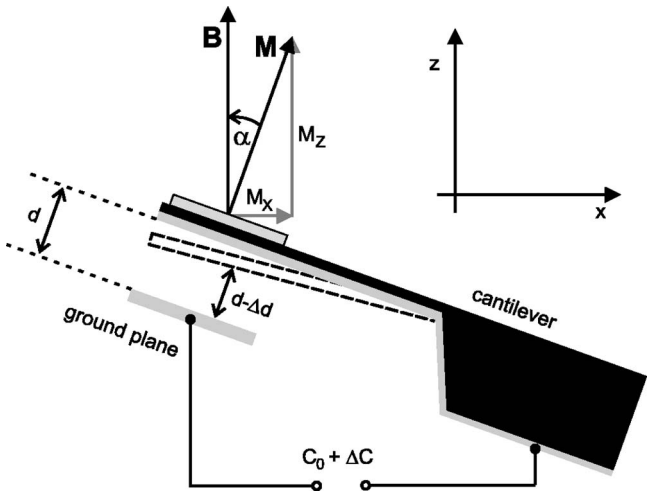

FIG. 1. Schematic side view of the cantilever magnetometer with an applied Si/SiGe sample. The cantilever normal is tilted by an angle α with respect to **B**. A torque $\boldsymbol{\tau}=\mathbf{M}\times\mathbf{B}$ is acting on an anisotropic magnetic moment **M**. The resulting cantilever deflection is detected with a capacitive readout scheme monitoring $C_0+\Delta C$ as a function of B. The separation d is about 100 μm in the experiment. Details of the technique are described in Refs. 10 and 11.

corresponding to the Landau quantization and to the spin splitting of Landau levels. In high magnetic fields we resolve in addition the splitting of the two conduction-band valleys as oscillations in the magnetization at odd ν. The energy gaps due to the spin and valley splitting are found to be enhanced by electron-electron interactions. We perform calculations based on a single-particle model DOS to quantitatively analyze the enhancement by comparison and to determine the residual level broadening. Measurements under different tilt angles between magnetic field and 2DES normal show that the size of the valley splitting is determined solely by the perpendicular magnetic field, while the spin splitting depends strongly on the total magnetic field. Additionally, we use the coincidence technique in dHvA measurements as a complementary means to determine the spin splitting. We will show that this technique is less affected by disorder broadening.

The paper is organized as follows: In Sec. II we briefly describe the experimental details. In Sec. III we analyze the dHvA effect—i.e., the magnetization oscillations in Si/SiGe that occur due to the Landau quantization and the spin and valley splitting of the DOS in a perpendicular magnetic field. In Sec. IV we focus on the effects of an additional strong parallel magnetic field. The method of coincidence experiments using the dHvA effect is introduced and evaluated in Sec. V. We discuss our results in Sec. VI and conclude with Sec. VII.

II. EXPERIMENT

Magnetization measurements were performed using micromechanical cantilever magnetometers fabricated from undoped GaAs heterostructures in a similar manner as described in Refs. 10 and 11 and sketched in Fig. 1. For measuring the magnetization of SiGe the samples were thinned to $\leqslant 10$ μm by wedging them from the backside and glued to cantilevers. Due to the anisotropic magnetic moment **M** of the sample in an external magnetic field **B**, a torque $\boldsymbol{\tau}=\mathbf{M}\times\mathbf{B}$ is exerted on the cantilever which can be measured capacitively.

TABLE I. Properties of sensors and samples.

	Sample 1	Sample 2	Sample 3
Torque resolution $\delta\tau[10^{-14}$ N m]	0.9	4.9–6.3	20.0
At tilt angle α	15°	15°–82°	15°
Mesa [mm^2]	1.26	1.14	1.01
$n_s[10^{11}$ cm^{-2}]	7.5	7.2	7.2

The magnetic field is chosen to point in the z direction—i.e., $\mathbf{B}=B\mathbf{e}_z$. The experiment is directly sensitive to the x component of the magnetization, M_x, which is perpendicular to **B**.

We have investigated three samples (Table I) from the same wafer grown by molecular beam epitaxy. In this heterostructure the 2DES resides in a 25-nm strained Si channel embedded between two $Si_{0.7}Ge_{0.3}$ barriers. The sample is doped with Sb in the top layer separated from the Si channel by a 12-nm spacer.[12] The 2DES forms in a triangular potential well at the interface between the strained Si and $Si_{0.7}Ge_{0.3}$ top barrier. Sample 1 was optimized for maximum sensor sensitivity at $B\leqslant 8$ T, providing access to detailed investigations of high-index Landau levels. Sample 2 was optimized for tilt-angle-dependent measurements in superconducting magnets, and sample 3 was optimized for operation in a high-field Bitter magnet at the HFML Nijmegen. Sensor optimization was achieved by adjusting the flexibility of the cantilever beam and the distance between the two electrodes forming the plate capacitor. High flexibility and small distance led to maximum sensitivity in the superconducting magnet. An increased stiffness and larger distance were useful for operation in Bitter magnets with their higher mechanical noise. The achieved torque resolution in the particular environment is given in Table I. We refer here to the torque resolution, since the resolvable magnetization signal δM depends on the magnitude and direction of the magnetic field via $\delta M=\delta\tau/(B_\perp \tan\alpha)$. The angle α is defined in Fig. 1. We assume that the absolute calibration of our sensors is accurate within ±5%.

A mobility $\mu=2\times10^5$ cm^2/(V s) at $T=0.3$ K was obtained from transport measurements on samples prepared from the same wafer. The electron sheet densities n_s evaluated from the magnetization oscillations are given in Table I. Temperature-dependent data were taken by placing the cantilevers on the cold finger of a vacuum loading ^{3}He system. Angle-dependent measurements were performed by placing the sample directly in the mixing chamber of a ^{3}He—^{4}He dilution refrigerator with a sample stage allowing for *in situ* rotation. In the presented data, the smooth background signal arising from the magnetization of the cantilever itself is removed from the experimental curves by subtracting a polynomial in $1/B_\perp$.

III. de HAAS–van ALPHEN EFFECT

For a magnetic field component $B_\perp$ perpendicular to an ideal 2DES, the energy level structure consists of a series of Landau levels with energies

$$E_j = (j + 1/2)\hbar\omega_c. \quad (1)$$

Here, $j=0,1,2,\ldots$ is the LL index and $\omega_c=eB_\perp/m^*$ is the cyclotron frequency. $m^*=0.19m_e$ is the transversal effective electron mass in Si. Each LL splits into two spin levels at energies $E_{j,s}=E_j+sg^*\mu_B B$, with $s=\pm 1/2$ and the effective Landé factor g^*. B denotes the total magnetic field here. For a 2DES in Si (100), where two conduction-band valleys are occupied, each spin level additionally consists of two distinct valleys. Each spin- and valley-split Landau level has a degeneracy $N_\nu=eB_\perp/h$. Increasing the magnetic field will successively depopulate the LL's and lead to steps in the magnetization.

We first focus on the data obtained for the small tilt angle $\alpha=15°$, where the influence of the parallel magnetic field component $B_\parallel$ on the level structure can be neglected. Figure 2 shows experimental magnetization curves of all three samples at low temperature T. Strikingly, we observe sawtoothlike dHvA oscillations of the magnetization which occur at even and odd filling factors $\nu=n_s/N_\nu$. The oscillations with peak-to-peak amplitudes ΔM at even integer filling factors $\nu=4(j+1)=4,8,12,16,20,\ldots$ reflect the chemical potential jumping across the energy gap ΔE between adjacent Landau levels. Oscillations arising from the spin splitting occur at $\nu=4j+2=2,6,10,14,18,\ldots$. Additional oscillations at odd filling factors $\nu=2j+1=3,5,7,9$ are in particular interesting since they arise from the lifting of the valley degeneracy in Si.

The data are displayed in units of effective Bohr magnetons $\mu_B^*=e\hbar/2m^*$ normalized to the total number of electrons. This calibration assumes that the oscillatory part of the dHvA effect arises only from the perpendicular component $M_\perp$ of the magnetization. The justification for this assumption will be discussed in Sec. IV. The dHvA amplitude of the ideal spin degenerate 2DES is $\Delta M=2\mu_B^*$ per electron at $\nu=4,8,\ldots$.

In the experiment, the dHvA effect at Landau filling factors becomes visible well below $B_\perp=1$ T. The amplitude ΔM is plotted in Fig. 3(a) as a function of $B_\perp$. It increases monotonically with increasing $B_\perp$, but even at high $B_\perp$ is much smaller than $2\mu_B^*=2\times 4.88\times 10^{-23}$ J/T. At $\nu=4$ the amplitude evaluates to $\Delta M_{\nu=4}=0.6\mu_B^*$. This apparent reduction of the LL gap will be discussed in detail later on.

Oscillations associated with the spin splitting of LL's can be observed up to $\nu=18$. ΔM increases strongly with magnetic field [Fig. 3(a)]. The amplitudes at spin filling factors $\nu=(4j+2)$ are evaluated after subtracting a linear function corresponding to the monotonous increase of M between the adjacent oscillations at $\nu=4j$ and $\nu=4(j+1)$. The dHvA amplitude at $\nu=2$ evaluates to $\Delta M_{\nu=2}\approx 0.6\mu_B^*$; i.e., it has the same size as $\Delta M_{\nu=4}$, demonstrating that the effective spin splitting is comparable to the LL separation in high magnetic fields.

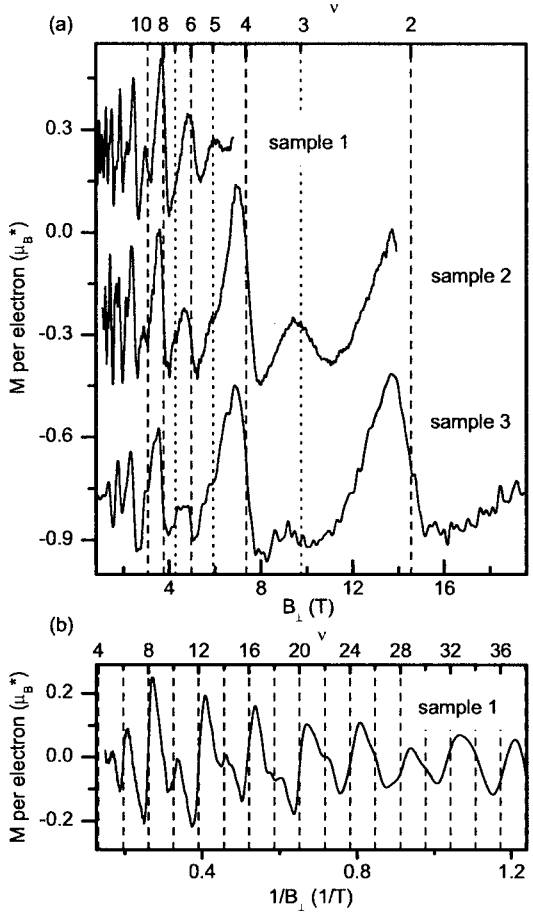

FIG. 2. (a) Experimental magnetization traces of sample 1 (upper curve) and sample 2 (middle) taken at $T=30$ mK in a superconducting magnet with $dB/dt=0.1$ T/min and of sample 3 (lower curve) measured at $T=400$ mK in a high-field Bitter magnet with $dB/dt=1$ T/min. Sharp magnetization oscillations that are due to Landau, spin, and valley gaps are clearly resolved. The smearing of the oscillations in the lower curve is due to the high ramp rate in the Bitter magnet and the signal averaging. The curves are offset for clarity. (b) To highlight the $1/B_\perp$ periodicity and to show the low-field behavior in more detail, the data for sample 1 are plotted versus the reciprocal field.

The dHvA effect at odd filling factors is observed up to $\nu=9$ in our measurements, thus providing clear evidence for the lifting of the valley degeneracy in the ground-state energy spectrum of the system. The corresponding amplitudes are smaller if compared to the Landau and spin splittings but increase sharply with $B_\perp$. Extrapolation of this trend suggests a valley splitting in the quantum limit at $\nu=1$ that might even be in excess of the spin splitting. For the evaluation, again a linear slope has been subtracted to account for the increase of M between the neighboring oscillations.

In order to get a direct quantitative access to the energy gaps from our magnetization data we can use the simplified Maxwell relation $\Delta M/N=\Delta E/B$ which holds for an ideal 2DES.[13] Here, N is the total number of electrons. The energy gap ΔE associated with the magnetization step ΔM is then given by

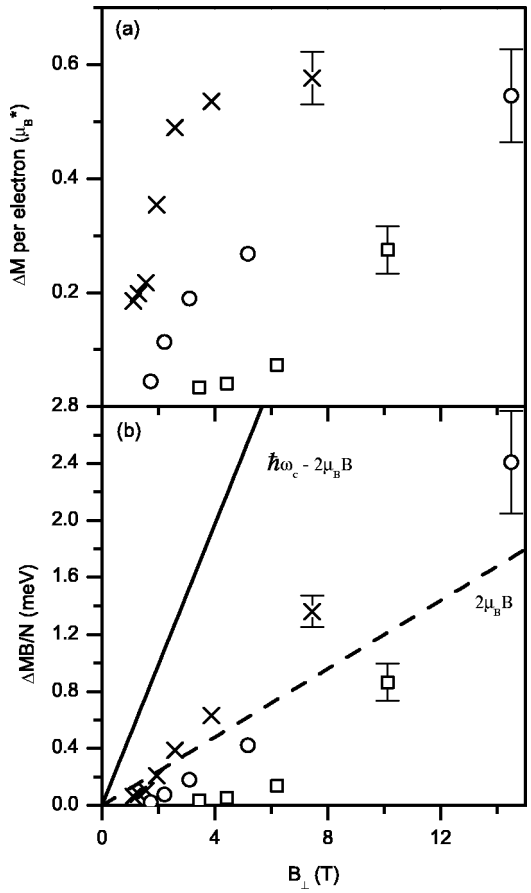

FIG. 3. (a) Peak-to-peak oscillation amplitudes ΔM for Landau ($\times$), spin ($\bigcirc$), and valley ($\square$) filling factors. (b) Energy gaps $\Delta E = \Delta MB/N$ recalculated from the measured amplitudes ΔM—i.e., without correcting for the level broadening. The dashed line shows the bare Zeeman energy $E_Z = 2\mu_B B$. The solid line denotes $\hbar\omega_c - E_Z$.

$$\Delta E = \Delta MB/N. \tag{2}$$

Note that this is a determination of the gaps directly from the magnetization jumps at a fixed temperature. In traditional transport measurements the gap is, in contrast, more indirectly deduced from temperature dependent Arrhenius plots.

Equation (2) has been used successfully in GaAs-based 2DES's to recalculate the level separations in a first approximation.[11,13,14] Following this approach we determine the energy gap ΔE between levels from the measured dHvA step size ΔM. The results are summarized in Fig. 3(b). The step size observed at $\nu = 4(j+1)$ corresponding to the transition from a spin-down higher LL to a spin-up lower LL indeed increases almost linearly with $B_\perp$. However, it stays well below the $\hbar\omega_c - \Delta E_Z$ line predicted for the ideal 2D system of noninteracting electrons. With a band-structure Landé factor $g=2$ and an effective mass $m^* = 0.19 m_e$, the Zeeman splitting $\Delta E_Z = g\mu_B B$ would reduce the energy splitting $\hbar\omega_c$ of two neighboring LL's with opposite spin by 20%. The energy gap extracted from the experimental data is much smaller, amounting to only 40% of $\hbar\omega_c - \Delta E_Z$. As we will show further on by means of temperature-dependent experiments this unexpected reduction of the LL gaps can be mainly attributed to disorder broadening and not to an increased m^* as suggested for magnetocapacitance data in Ref. 3.

To evaluate the dHvA effect at Landau filling factors in more detail, calculations based on a model DOS have been applied with great success for GaAs heterostructures.[11,15–18] Here, the shape of the DOS was found to be well approximated by Gaussian- or Lorentzian-broadened LL's at $E_{i,j}$ and an energy-independent background DOS. The magnetization $M = -(\partial F/\partial B)|_{N,T}$ was calculated from the assumed DOS via the free energy F and the condition of constant electron number (see Ref. 11 for details). In case of the Si/SiGe system we find from Figs. 2 and 3 that the relevant energy scales for the different energy splittings are all of the same order of magnitude, leading to a more complex situation for modeling than in the GaAs system. Since the experimental magnetization signal ΔM at spin and valley filling factors is dominated by exchange effects, as will be discussed later, a DOS model assuming noninteracting electrons cannot account for the details of the observed magnetization curves. However, evaluations for the low- and intermediate-field ranges can be made.

In order to successfully model the magnetization traces at $\nu = 4(j+1)$ in this range we have assumed a Gaussian-broadened DOS with broadening parameter $\Gamma = 0.15$ meV $\times B_\perp$ [T]$^{1/2}$ and a background DOS of 30% of the zero-field DOS $D_0 = m^*/\pi\hbar^2$. Such simulations are later used as an independent means to recalculate the intrinsic spin splitting by taking into account the disorder broadening Γ of the LL's. In Fig. 4 we show measured and simulated magnetization data. The dashed line denotes the magnetization trace for $g=2$—i.e., taking into account only the single-particle Zeeman splitting. The solid line is the result of a calculation that incorporates an oscillating Landé factor g^* in a phenomenological way. Two things are striking here: (I) The amplitude at *Landau* filling factors is altered significantly by changing the behavior of g^* at *spin* filling factors. The dHvA effect due to Landau quantization and due to the spin splitting of LL's can thus not be analyzed independently from each other. (II) Even the model with an oscillating g^* reaching $g^* \approx 3$ at $\nu = 14$ fails to describe the sharp sawtoothlike oscillation seen in the experiment. Clearly, a fully self-consistent calculation including electron-electron interactions is needed to quantitatively model the dHvA effect in Si/SiGe quantum wells. Such a model is beyond the scope of this paper.

The spin gap recalculated from the ΔM data is shown in Fig. 3(b). For $\nu \geqslant 6$ the values stay well below E_Z (dashed line); i.e., no enhancement of the gap is observed. For $\nu = 2$, however, ΔE is far larger than the expected $2\mu_B B$ for Si. The enhancement of ΔM corresponding to a spin gap value greater than the single-particle Zeeman splitting ΔE_Z is well known for 2DES's in GaAs and attributed to exchange interactions.[11,19] The effective energy splitting ΔE_s is then composed of two terms $\Delta E_s = \Delta E_Z + E_{ex}$, where E_{ex} is expected to scale with the Coulomb energy E_C. An effective Landé factor g^* is often used to parametrize this energy gap. At $\nu = 2$ we find an energy gap $\Delta E = 2.9\mu_B B$; i.e., an enhancement corresponding to $g^*_{\Delta M} = 2.9$ is found. Here, the notation $g^*_{\Delta M}$ is introduced to avoid confusion with the values deter-

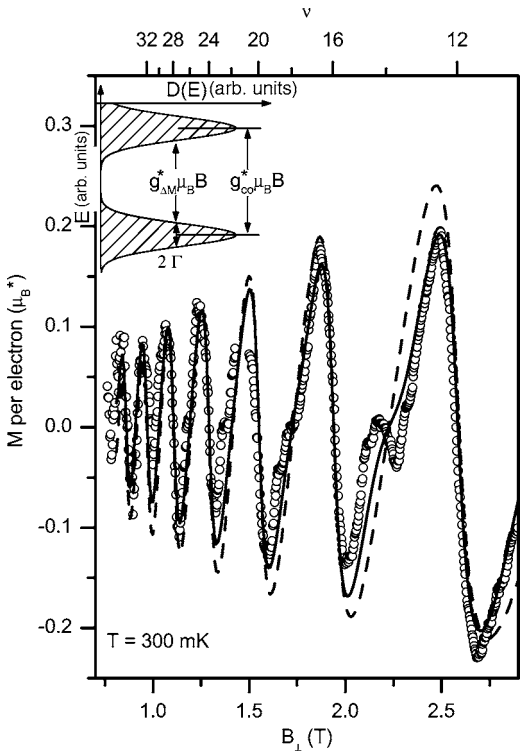

FIG. 4. Comparison of experimental magnetization and model calculation in the low-field regime. The open symbols denote the experimental magnetization trace of sample 1 at $T=300$ mK. A smooth background has been subtracted from the data. The lines represent the result of model calculations with a Gaussian-broadened DOS with $\Gamma=0.15\ \mathrm{meV}\times B_\perp\ [\mathrm{T}]^{1/2}$ and an energy-independent background of 30% of the zero-field DOS. The dashed line denotes the magnetization trace for $g=2$—i.e., taking into account only the single-particle Zeeman splitting—while the solid line is the result of a calculation that incorporates an oscillating g^* in a phenomenological way. Inset: sketch of a DOS with disorder-broadened LL's and the definition of parameters.

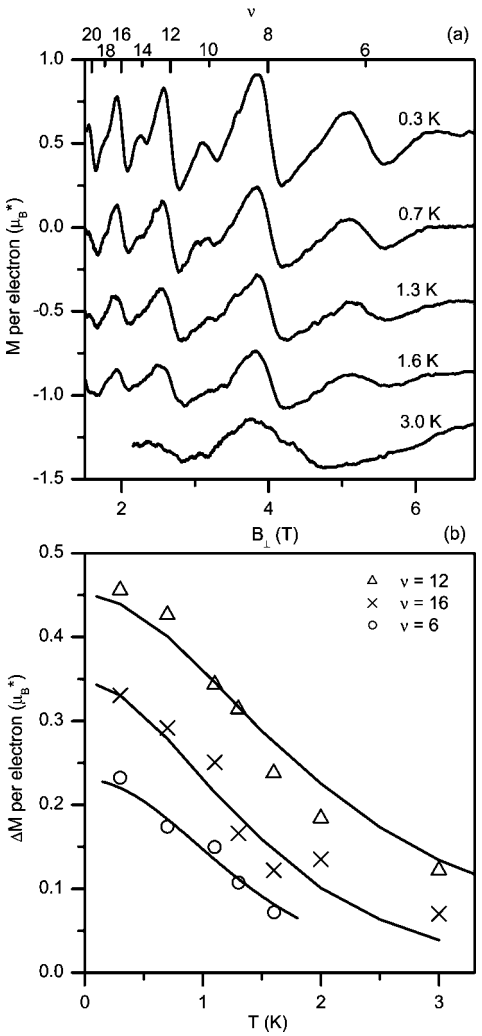

FIG. 5. (a) Experimental magnetization of sample 1 measured at different temperatures. Curves are offset for clarity. (b) Temperature dependence of the peak-to-peak dHvA amplitude ΔM at Landau filling factors $\nu=12$ and $\nu=16$ and spin filling factor $\nu=6$. The experimental values are indicated by symbols; the results of the model calculations are denoted by solid lines. For modeling ΔM at $\nu=6$ we assumed $g^*=3.2$ with level broadening $\Gamma=0.15\ \mathrm{meV}\times B_\perp\ [\mathrm{T}]^{1/2}$.

mined by the coincidence measurements, denoted g^*_{co}, in Sec. V. $g^*_{\Delta M}$ includes directly the disorder present in the system. This is illustrated schematically in the inset of Fig. 4: From ΔM one extracts an energy gap value that is reduced by the level broadening Γ. The coincidence technique in contrast yields the energetic distance between the *centers* of LL's. Note, however, that both values reflect renormalized energy gaps including all interaction effects.

Modeling the magnetization traces with a fixed value for g^* and considering the broadening parameter $\Gamma=0.15\ \mathrm{meV}\times B_\perp\ [\mathrm{T}]^{1/2}$ we find that $g^*=5$ models the experimentally observed ΔM at $\nu=2$. These two estimates of g^* for $\nu=2$ already indicate that Coulomb exchange interactions can considerably enhance the spin gap and the corresponding dHvA step size as was observed earlier on 2DES's in GaAs.[11,13,19] The spin splitting will be discussed further along with the angle-dependent data in Sec. IV.

The energy gaps extracted from ΔM at odd ν yield the size of the valley splitting of a given spin level and are the smallest values in Fig. 3(b). They increase strongly with magnetic field for $B_\perp>6$ T. At $\nu=3$ we find a valley gap $\Delta E_V=0.8$ meV which is far larger than the splitting ≈ 0.1 meV predicted in the noninteracting electron picture.[20,21]

Experimental magnetization curves for sample 1 measured at different temperatures are shown in Fig. 5(a), and ΔM vs T is summarized in Fig. 5(b). The sawtoothlike dHvA effect observed at $T=300$ mK diminishes fast when the temperature is increased. Oscillations at $\nu=4j+2=6,10,14$ are already smoothed out at $T\sim 2$ K, while oscillations at $\nu=4(j+2)=8,12$ remain visible above $T\sim 3$ K. To extract additional information on the size of the energy gaps from ΔM vs T in Fig. 5(b) we performed temperature-dependent model calculations. The solid lines denote the calculated T dependences resulting from the DOS model. From this we can also evaluate the corresponding energy gap. This method is complementary to Eq. (2). In particular, the actual size of the energy gap and the influence of the disorder broadening

can be separated in this analysis. The good agreement between calculation and experiment in Fig. 5(b) shows that the Landau energy gap corrected for the effect of disorder broadening is indeed of the size $\hbar\omega_c - \Delta E_Z$ with $m^* = 0.19 m_e$ and $g=2$ for the spin-unpolarized 2DES. The discrepancy in Fig. 3(b)—that $\Delta MB/N$ falls below the line indicating the behavior of the ideal system—can thus be attributed to the level broadening Γ. It shows that disorder has a dominant influence on the electronic energy spectrum in the high-mobility SiGe heterostructures. This is in contrast to, e.g., high-mobility GaAs 2DES's, where the energy gaps between LL's and the corresponding dHvA amplitudes were shown to be very close to the value of the ideal 2DES.[11]

IV. ANGULAR DEPENDENCE OF THE MAGNETIZATION

As already mentioned at the beginning of the previous section, the Landau-level separation is determined merely by the perpendicular field component $B_\perp$ whereas the spin splitting ΔE_Z is governed by the total magnetic field B. In order to access the interplay of these competing energy scales we have performed magnetization experiments in magnetic fields **B** tilted with respect to the normal of the 2D plane. As depicted in Fig. 1, z is defined by the direction of $\mathbf{B} = B\mathbf{e}_z$. The perpendicular and normal components with respect to the 2D plane are denoted by $\perp$ and $\parallel$, respectively. Experimental data shown in Fig. 6 are obtained by tilting the 2DES normal away from the z direction. Here, the magnetization component $M_\perp$ perpendicular to the 2DES is shown as a function of the perpendicular magnetic field component $B_\perp$. In this presentation the positions of integer filling factors remain fixed for different tilt angles, since N_ν depends only on $B_\perp$.

The torque experiment measures M_x (cf. Fig. 1). For the case of a real 2DES with finite thickness in a tilted magnetic field the magnetization vector is not expected to point strictly perpendicularly to the electron sheet. For that reason the absolute size and direction of **M** cannot be recalculated from M_x alone in this more general case. We can, however, assume safely that the sawtoothlike dHvA oscillations occur only in the perpendicular component $M_\perp$. The main argument for this is that the confinement potential in the growth direction—i.e., in the $\perp$ direction—is so large compared to the magnetic confinement that a diamagnetic shift of the energy levels occurs by means of the in-plane component $B_\parallel$ but no Landau quantization. The latter is reasonable as long as the magnetic length l_B is larger than the thickness of the 2DES, which is true for the field range $B_\parallel \leqslant 16$ T used in the experiments. A more detailed discussion is given in Ref. 22.

Following these arguments the abrupt jumps of the dHvA effect occur only in $M_\perp$ and we can identify the oscillatory part of the measured magnetic moment with the oscillatory part of $M_\perp$. This allows for a calibration of our data in absolute units using $M_\perp = M_x/\sin\alpha$.

In Fig. 6, $M_\perp$ is shown for tilt angles between $\alpha=35°$ and $\alpha=72.3°$. We first focus on filling factors $\nu \geqslant 8$. Here the valley splitting can be neglected. As in a (nearly) perpendicular field, steps in the magnetization occur at fixed $\nu=4(j+1)$ and $\nu=4j+2$ and can be related to transitions between LL's with opposite spin or between two spin levels within the same LL, respectively. Using Eq. (2), which is also valid in tilted magnetic fields, we can again relate the magnetization steps to energy gaps between two neighboring levels:

$$\Delta E = \frac{\Delta M_\perp B_\perp}{N}. \tag{3}$$

The evolution of $\Delta M_\perp$ with α thus directly reflects the angular dependence of the energy gap ΔE between levels in the DOS.

The $\alpha=35°$ curve shows pronounced dHvA oscillations at Landau filling factors $\nu=4(j+1)$ and well-resolved oscilla-

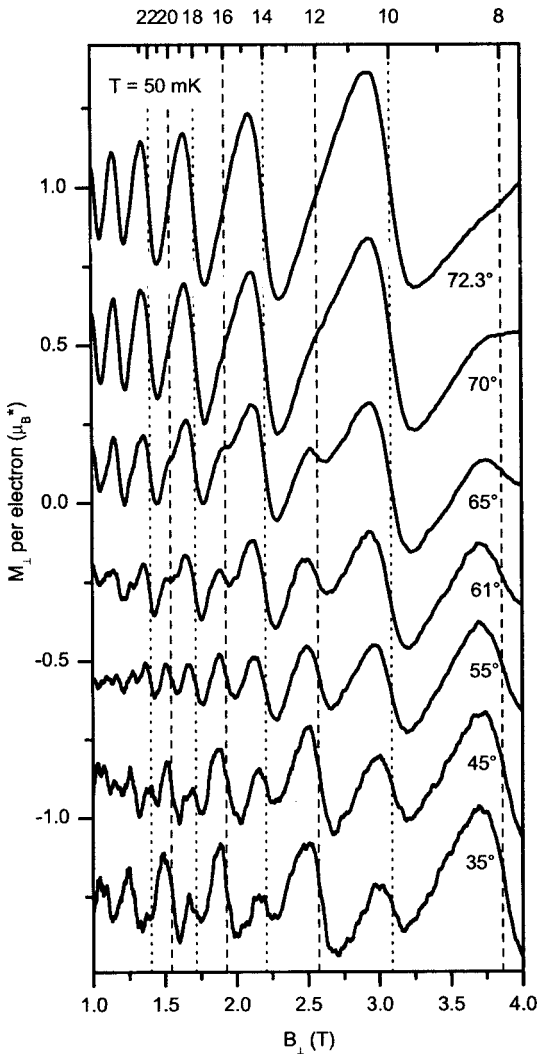

FIG. 6. Experimental magnetization of sample 3 for specific tilt angles α. α increases from bottom to top. To illustrate the coincidence effect at 72.3°—i.e., the vanishing of dHvA oscillations at certain integer ν—we present the angle-dependent data as a waterfall plot where each curve is offset for clarity. The sample was rotated *in situ*, and data were taken at $T=50$ mK. Around $\alpha=50°$ the amplitude ΔM is nearly the same for all filling factors. The 72.3° curve shows the magnetization at the first coincidence—i.e., where $g^*\mu_B B = \hbar\omega_c$. Data for $\alpha > 72.3°$ are shown in Fig. 7(a).

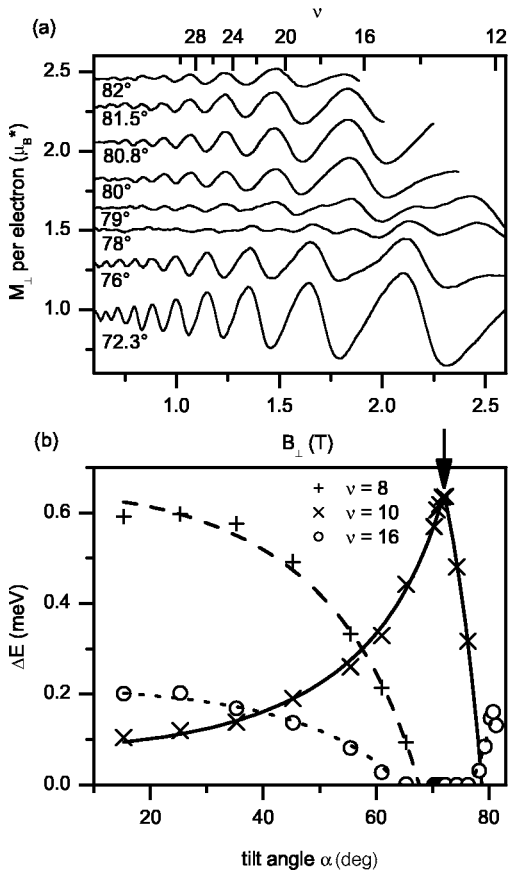

FIG. 7. (a) Experimental magnetization traces at specific angles $\alpha \geqslant 72.3$ (α increases from bottom to top). At $\alpha=80.8$ the second coincidence condition is met. (b) Energy gaps at Landau filling factors $\nu=8$ (+) and $\nu=16$ (○) and at spin filling factor $\nu=10$ (×). The spin gap increases monotonically up to a maximum value $\Delta E_{\nu=10}=0.65$ meV at $\alpha=72.3°$ (arrow). Here two spin levels of opposite spin orientation from adjacent Landau levels coincide—i.e., $g^*\mu_B B=\hbar\omega_c$. For $\alpha>72.3°$ the spin gap decreases fast and goes to zero. The second coincidence condition $g^*\mu_B B=2\hbar\omega_c$ is met at 80.8°. The solid line is a best fit for the functional form $f(\alpha)=a/\cos\alpha+b$ and describes the data within the experimental accuracy. At $\nu=10$, we get $a=0.25$ meV and $b=-0.17$ meV. The Landau gaps show the inverted behavior, and their dependence on α can be described by choosing a negative value for a.

tions with smaller amplitude at spin filling factors $\nu=4j+2$. With increasing α the amplitude $\Delta M_\perp$ at the spin filling factors increases while $\Delta M_\perp$ at Landau fillings decreases. At $\alpha\approx 50°$ both Landau and spin oscillations have the same amplitude. For higher α, $\Delta M_\perp$ at $\nu=4j+2$ exceeds the amplitudes at $\nu=4(j+1)$, until at $\alpha=72.3°$ the oscillations at Landau filling factors have vanished and $\Delta M_\perp$ at spin filling factors is at maximum. For even higher tilt angles [Fig. 7(a)] this behavior reverses: The amplitude at $\nu=4j+2$ decreases towards zero and the amplitude at Landau filling factors increases towards a maximum.

This behavior can be explained by the different dependence of the Zeeman and the cyclotron energy on the magnetic field. In the ideal case of an infinitely thin 2DES the parallel field component $B_\parallel$ couples to the electron system only via the Zeeman splitting $\Delta E_Z=g\mu_B B$. This energy gap increases with increasing tilt angle. The effective spin gap which is measured via the dHvA amplitude is then given by

$$\Delta E_s=\Delta E_Z\left(\frac{B_\perp}{\cos\alpha}\right)+E_{ex}(B_\perp)-2\Gamma(B_\perp)\approx g^*_{\Delta M}\mu_B B. \quad (4)$$

The effective Landau gap is reduced by the neighboring spin gaps—i.e.,

$$\Delta E_L=\hbar\omega_c(B_\perp)-\Delta E_Z\left(\frac{B_\perp}{\cos\alpha}\right)-2\Gamma(B_\perp). \quad (5)$$

By changing the angle one can thus tune the relative size of the spin and Landau splitting. The evolution of the corresponding energy gaps recalculated from the magnetization data in Figs. 6 and 7(a) is displayed in Fig. 7(b) for $\nu=8,10,16$. The spin gap at $\nu=10$ increases monotonically with α up to a maximum value (arrow). At this point the effective spin splitting $g^*\mu_B B$ equals $\hbar\omega_c$; i.e., the levels coincide. This situation is referred to as the first-order coincidence. The effective Landau splitting (+,○) vanishes at this point. For $\alpha>72.3°$ the spin gap decreases fast and approaches zero when the second coincidence condition $g^*\mu_B B=2\hbar\omega_c$ is met. Here, the Landau gaps exhibit a local maximum as function of α. The evolution of the energy gaps at fixed filling factor—i.e., fixed $B_\perp$—can be described by a phenomenological function $f(\alpha)=a/\cos\alpha+b$ shown as lines in Fig. 7. $f(\alpha)$ models the functional form of Eq. (4), and a evaluates to about $0.7E_Z$ for $\nu=10$. The value of b is dominated by the level broadening Γ.

In order to shed further light on the angular dependence of the spin gap we modify the representation of Eq. (4) by introducing an extra free parameter Δs:

$$\Delta E_s=\Delta s|g|\mu_B B+E_{ex}(B_\perp)-2\Gamma(B_\perp). \quad (6)$$

In Fig. 8 we plot ΔE_s versus the Zeeman energy, both in units of the exchange energy E_C. The dimensionless parameter $\tilde{g}=E_Z/E_C$ is both proportional to $B_\perp^{1/2}$ and to $1/\cos\alpha$. The data for a fixed ν are well fitted by a linear function. The corresponding slopes Δs for a given ν are summarized in the inset. They follow a linear trend as a function of ν instead of being constant at $\Delta s=1$. We find a systematic deviation from $\Delta s=1$ of the ideal system in our experiment for all resolved filling factors. Possible reasons for this will be discussed in Sec. VI.

Leaving the analysis of the spin splitting we now turn to a direct experimental determination of the valley splitting in a tilted magnetic field. For this we have plotted the evolution of the dHvA effect at $\nu=5$ in Fig. 9(a). The evolution of the corresponding valley energy gap (●) is shown in Fig. 9(b) together with the gaps at Landau and spin filling factors. The striking result is that $\Delta E=\Delta M_\perp B_\perp/N$ at $\nu=5$ remains nearly constant as a function of α. This provides clear evidence that the valley splitting does not depend on the total magnetic field B but is rather governed by the normal field component only.

V. FIRST AND SECOND COINCIDENCE

By adjusting the tilt angle the 2DES can be tuned to conditions where the energetic positions of different levels coin-

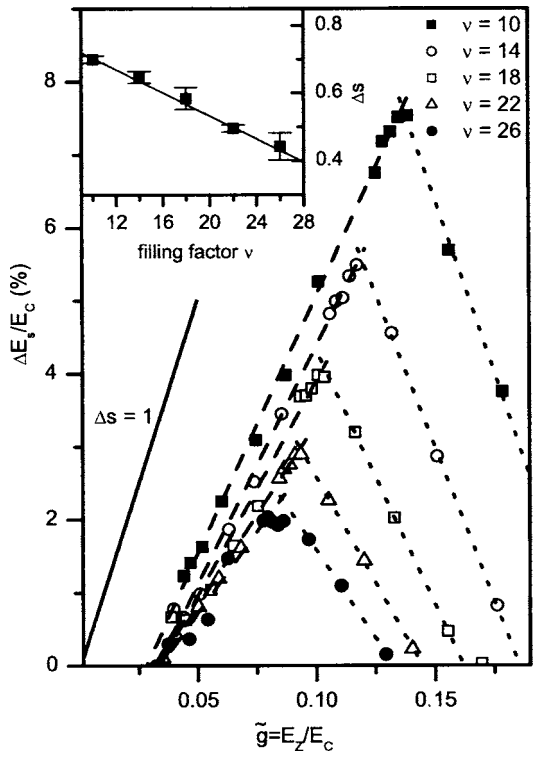

FIG. 8. Measured spin energy gap normalized to the Coulomb energy E_C vs $\tilde{g}=E_Z/E_C$. $\Delta s=1$ modeling the ideal 2DES is shown as a solid line for comparison. The slopes Δs of the linear fits (dashed lines) are summed up in the inset. Their deviation from $\Delta s=1$ indicates an additional angular dependence of the energy gap apart from that given by the Zeeman energy.

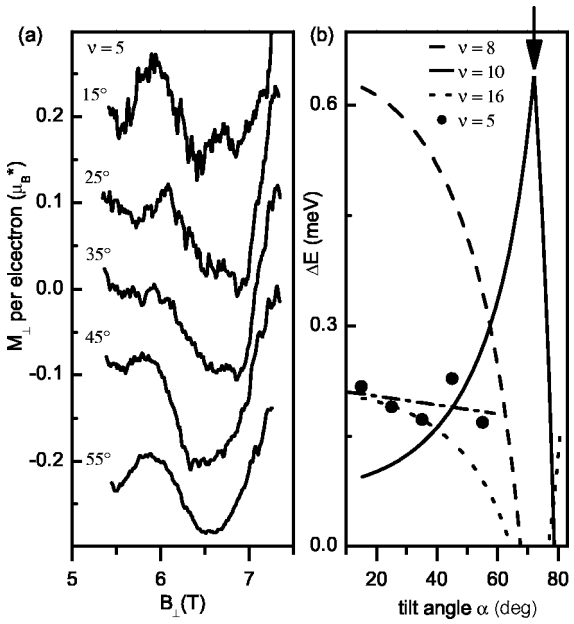

FIG. 9. (a) dHvA oscillation at valley filling factor $\nu=5$ for different tilt angles α. Curves are offset for clarity. The angle increases from top to bottom. The oscillation amplitude and hence the energy gap at $\nu=5$ depend only weakly on the tilt angle. (b) Recalculated energy gaps vs angle for Landau, spin, and valley filling factors. Solid circles mark the energy gaps at $\nu=5$ recalculated from the dHvA oscillations in (a). The dash-dotted line is a guide to the eye.

cide (Fig. 10). As will be described in the following this coincidence technique can be used to gain information about the electronic level structure that is complementary to that extracted from the absolute values of the dHvA amplitudes alone. The technique is well established in magnetotransport experiments as a means to determine the effective Landé factor g^*.[23–25] Here, we introduce the coincidence technique to the field of dHvA effect studies. We will limit the following analysis to the filling factor range $\nu \geqslant 9$. In this regime the valley splitting is not resolved in our measurements. Since g^* enhanced by exchange interaction is an oscillatory function of B (cf. Ref. 26), the coincidence conditions can be quite involved and it is worth discussing them in detail.

The energy levels of the ideal 2DES in a tilted field are given by

$$E_{j,s} = (j + 1/2)\frac{\hbar e B_\perp}{m^*} + s g^* \mu_B B. \tag{7}$$

For a constant g^* this leads to a coincidence of the spin-up and spin-down levels of different Landau levels whenever the condition

$$g^*_{co}\mu_B B \doteq p\hbar\omega_c, \quad p = 1,2,3,\ldots, \tag{8}$$

is satisfied. Here, a g^*_{co} is introduced to distinguish the result of the coincidence technique from $g^*_{\Delta M}$ in Sec. III. The evolution of the level structure as a function of $B/B_\perp = 1/\cos\alpha$

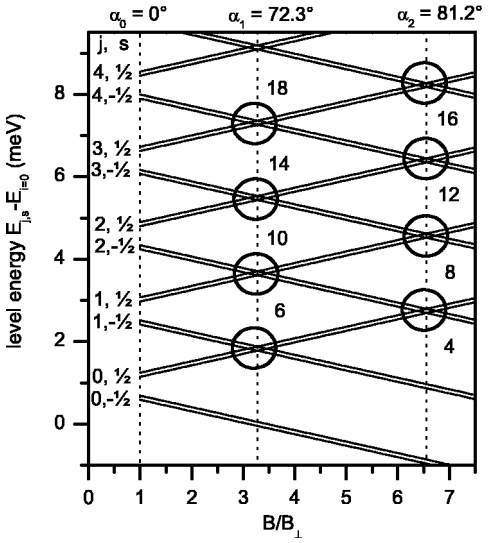

FIG. 10. Sketch of the energy levels for a 2DES in Si as a function of $B/B_\perp = 1/\cos\alpha$, illustrating the effect of coinciding levels. $B_\perp$ is fixed at 3 T. The circles mark coincidence positions where $g^*\mu_B B$ equals integer multiples of $\hbar\omega_c$. The numbers indicate the filling factors where a *maximum* dHvA amplitude should occur. The valley splitting is assumed here to be field independent and small compared to the Landau and the Zeeman splitting. This is justified since we limit the coincidence analysis to the regime $\nu \geqslant 9$, where the valley splitting is not yet resolved experimentally.

is illustrated schematically in Fig. 10 for a constant $g^*=3.2$ at a constant perpendicular field $B_\perp=3$ T. In a perpendicular field ($\alpha=0°$) ΔE_Z is about one-third of $\hbar\omega_c$. With increasing α the spin-up levels move to higher relative energies while the spin-down levels move downwards. At $\alpha_1=72.3°$ the spin splitting equals the Landau splitting and the levels $E_{j,1/2}$ and $E_{j+1,-1/2}$ coincide. The positions of the level crossings are marked by circles in Fig. 10. Increasing the angle further leads to higher-order coincidences when ΔE_Z equals integer multiples of the Landau splitting.

This simple picture is modified in an interacting electron system since the enhanced g^* is supposed to depend on the relative populations of the spin-up and spin-down levels within a given Landau level; i.e., it depends on the position of the Fermi energy. The expression for the effective spin splitting of the jth Landau level in the Hartree-Fock approximation is given by[27,28]

$$E_{j,1/2} - E_{j,-1/2} = |g|\mu_B B + E_C \sum_k X_{j,k}(\nu_{k,1/2} - \nu_{k,-1/2}), \quad (9)$$

where $\nu_{k,s}$ is the partial filling of the level (k,s) and the coefficients $X_{j,k}$ are obtained by integrating the matrix elements of the Fourier transform of the Coulomb potential. The *maximum* enhancement of the spin gap is thus given when E_F lies *between* spin-split states of the same Landau level, since here the difference of the partial fillings has its maximum. This situation is given at the fillings $\nu=4j+2$ for the first coincidence—i.e., $p=1$ in Eq. (8) and at $\nu=4(j+1)$ for the second coincidence ($p=2$). Evaluating the angle at which a maximum oscillation amplitude occurs at these filling factors thus yields the maximum g^*_{co}. Experimentally we find the first coincidence in Fig. 6 at

$$\alpha = (72.3 \pm 0.25)^\circ \Rightarrow g^*_{co} = (3.21 \pm 0.05) \quad (10)$$

for $\nu \geqslant 10$. The second coincidence [Fig. 7(a)] is observed at

$$\alpha = (80.8 \pm 0.25)^\circ \Rightarrow g^*_{co} = (3.38 \pm 0.05) \quad (11)$$

for $\nu \geqslant 16$. We find that g^*_{co} is larger at higher tilt angle. This is in agreement with the expectation and earlier transport measurements on the same type of sample:[29] According to Eq. (9) one would expect a larger g^* value at the second coincidence, since here the spin population difference is at maximum for *two* Landau levels. Furthermore, we find that $\Delta M_\perp$ has its maximum for all $\nu=4(j+1)\geqslant 16$ at the same angle; i.e., we extract the same value $g^*_{co}=3.38$ for all resolved filling factors. The same applies to the first-order coincidence where we find a field-independent $g^*_{co}=3.21$. In Fig. 11 the magnetization traces for the first and second coincidences are directly compared. Oscillations are clearly resolved up to $\nu=52$. In the $\alpha=72.3°$ trace (solid line) the dHvA effect occurs at $\nu=4j+2$ while oscillations at $\nu=4(j+1)$ are missing. The $\alpha=80.8°$ trace (dashed line) exhibits the inverted behavior as expected from the level scheme in Fig. 10. Striking in this direct comparison is that the peak-to-peak amplitudes are ~30% smaller for the second coincidence. This is attributed to the finite thickness of the 2DES and the effect of the in-plane field.

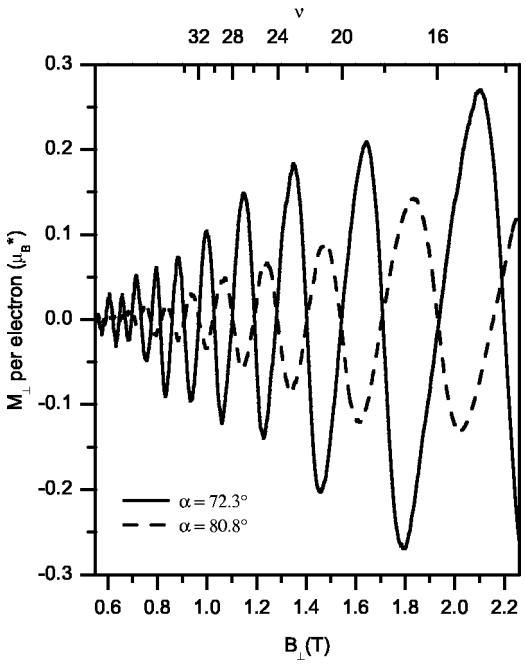

FIG. 11. Experimental magnetization $M_\perp$ vs $B_\perp$ for the first and second coincidence conditions. Where the first coincidence condition $g^*_{co}\mu_B B=\hbar\omega_c$ is met oscillations occur only at $\nu=4j+2$ and are suppressed at $\nu=4(j+1)$. At the second coincidence oscillations occur only at $\nu=4(j+1)$ while $M_\perp$ increases linearly at $\nu=4j+2$. Note the different dHvA amplitudes for the two cases.

VI. DISCUSSION

A. Landau filling factors

The energy gap corresponding to the transition from a spin-down higher LL to a spin-up lower LL recalculated from the dHvA amplitude evaluates to about 40% of $\hbar\omega_c-2\mu_B B$. By means of temperature-dependent measurements we could attribute this effect largely to level broadening. Our observation of a strongly reduced gap value is similar to the observations in Ref. 3, where the authors found a comparable reduction by magnetocapacitance measurements on Si MOSFET's. They argued that this effect is due to a renormalization of the effective mass and the g factor due to electron-electron interactions. Our analysis of temperature-dependent magnetization data suggests, however, disorder as the main reason, since the experimental T dependence, which yields a gap value that is corrected for the level broadening, is well described by a gap size $\hbar\omega_c-\Delta E_Z$ with $m^*=0.19m_e$ and $g=2$.

The *Landau-level broadening* at $\nu=4(j+1)$ was modeled by a Gaussian distribution with $\Gamma=0.15\ \text{meV}\times B_\perp\ [\text{T}]^{1/2}$. The self-consistent Born approximation by Ando and Uemura[30] predicts a semielliptical line shape with $\Gamma=(\hbar e/m^*)(2B_\perp/\pi\mu)^{1/2}$. Using the zero-field mobility determined from magnetotransport yields $\Gamma=0.11\ \text{meV}\times B_\perp\ [\text{T}]^{1/2}$, which is in good agreement with the result of our model. The remaining discrepancy might be due to the fact that the theory of Ando assumes short-range scattering, while earlier transport experiments in high-mobility Si/SiGe showed that the resistance is dominated by long-range scattering.[5]

In order to analyze the traces quantitatively over the full field range a model that self-consistently includes interaction effects is needed. From the experimental point of view, 2DES's of even higher mobility are needed in order to be able to quantify the effect of disorder on the electron-electron interaction in Si/SiGe heterostructures.

B. Spin splitting: Angular dependence

The *angular dependence* of the energy gaps shown in Fig. 8 yields $\Delta s < 1$; i.e., the variation of ΔE_s with $1/\cos\alpha$ is smaller than that given by the Zeeman energy. One may tentatively attribute this to a finite-thickness effect. Two observations are now particularly interesting: (I) Δs is constant for a given filling factor; i.e., the decrease of ΔE_s has exactly the same angular dependence as the Zeeman energy within the experimental accuracy. (II) Δs depends linearly on ν; i.e., the additional decrease of the gap is stronger for higher filling factors. This is the opposite of what is expected from coupling to the second subband: The decrease of the gap due to level coupling should be strongest for high B—i.e., low filling factors. Level mixing seems thus unlikely as an explanation. Incomplete spin polarization due to overlap of the disorder broadened levels should lead to larger slopes $\Delta s \geqslant 1$. However, a dependence of the level broadening Γ on the parallel magnetic field component $B_\parallel$ would explain the observed behavior at least qualitatively, since an increased level broadening has a stronger effect on high filling factors, where the intrinsic level separation is small. In Ref. 31 such a dependence was suggested, because the parallel-field-induced Lorentz force pushes the electrons in the 2DES towards the interfaces. As a result scattering by interface roughness or charged centers near the interface may be enhanced in a high parallel field.

Linear extrapolation of Δs as a function of ν in the inset of Fig. 8 suggests that Δs stays below $\Delta s = 1$ even in the quantum limit. In 2DES's in GaAs $\Delta s \simeq 7$ was found at $\nu = 1$ for $\tilde{g} \sim 0.01$ and interpreted as evidence for large-spin Skyrmionic excitations.[32] This regime was not reached in our experiment.

C. Coincidence measurements

One of our most striking results requiring some discussion is probably the enhancement of the g factor in our coincidence experiments. Our dHvA results compare very accurately with data obtained from magnetotransport experiments on samples from the same wafer as investigated here.[8,33] However, some striking differences have to be established: In the magnetotransport experiments by Zeitler *et al.*[8,33] the first coincidence is marked by the point where the Shubnikov–de Haas (SdH) minima in ρ_{xx} at $\nu = 4(j+1)$ have changed into maxima. The reported value for the first coincidence is $g^* = 3.18$. At these filling factors $\nu = 4(j+1)$ two levels overlap in the coincidence with E_F located in the center of these levels. Both are half-filled with electrons. Therefore the spin population difference is only half as large as possible, suggesting a smaller g^*_{co} according to Eq. (9). In contrast, in our dHvA measurements the coincidence condition is extracted from the angle where $\Delta M_\perp$ reaches a maximum at $\nu = 4j+2$. In this situation E_F is located *between* different spin levels of the same Landau level. This yields a *maximum* spin population difference and therefore a maximum g^* in Eq. (9).

In the light of the fact that the g^* extracted from magnetotransport and dHvA at different level occupancies are precisely the same, an interpretation of the g^* enhancement given by Eq. (9) seems to be rather puzzling. Additionally both experiments consistently yield $g^*_{co} = 3.21 = \text{const}$ for $\nu \geqslant 10$. It is well established experimentally that the single-particle band-structure g factor in this type of heterostructure is very close to $g = 2$, as has been confirmed by electron spin resonance experiments.[34,35] It is therefore clear that our experiment yields the enhanced Landé factor g^*. The different filling conditions—i.e., different spin level occupancies—do not really influence the size of this enhancement. It has to be noted that the validity of Eq. (9) in the case of the strongly interacting electron system in Si $(E_C/\hbar\omega_c > 1)$ is questionable.[3] One may speculate that 2DES's with higher mobility, where the effects of electron-electron interactions should be even more pronounced, could enlighten this point.

Direct recalculation of the spin energy gap from $\Delta M_\perp B_\perp / N = g^*_{\Delta M} \mu_B B$ and the evaluation of g^*_{co} from the coincidence reflect physically different quantities. In particular, the former yields a gap in the density of states that is reduced by the effect of level broadening, while the latter reflects the gap between the centers of mass of the levels. In order to illustrate this point, we have added subscripts to g^* representing the two different methods how g^* is determined. Evaluation of the oscillation amplitude provides $g^*_{\Delta M} = 1.1$ at $\nu = 10$ while the first coincidence gives $g^*_{co} = 3.21$. Assuming that the difference is due to level broadening we can estimate Γ from the condition $(g^*_{co} - g^*_{\Delta M})\mu_B B = 2.11\ \mu_B B[\nu = 10] \approx 2\Gamma$. This yields $\Gamma = 0.11\ (\text{meV}/\sqrt{\text{T}}) \times \sqrt{3.1\ \text{T}} = 0.19$ meV at $B_\perp = 3.1$ T. This value is consistent with the broadening $\Gamma = 0.15\ \text{meV} \times \sqrt{B_\perp\ [\text{T}]}$ obtained from the model calculations.

The recalculation of the energy gaps $\Delta E = \Delta M_\perp B_\perp / N$ from the dHvA amplitudes ΔM versus tilt angle α provides complementary information that is not accessible with the coincidence technique. Our observation of a systematic deviation of Δs from $\Delta s = 1$ shows that $B_\parallel$ couples not only through E_Z to the electron system; i.e., the conditions used for the interpretation of the coincidence measurements are not exactly fulfilled. This is particularly striking in Fig. 11 where the traces for the first and second coincidences are shown together: The amplitudes ΔM are much smaller for the second coincidence, indicating that the energy gaps are diminished by the increasing parallel magnetic field component.

D. Valley splitting

The *valley splitting* observed in high magnetic field is far larger than predicted in a picture of noninteracting electrons in Refs. 20 and 21:

$$\Delta E_V\ [\text{meV}] \approx 0.015(j + 1/2) B_\perp\ [\text{T}]. \tag{12}$$

Since the Landau index j decreases when $B_\perp$ is increased, the predicted valley splitting depends only weakly on $B_\perp$ and

is of the order of 0.1 meV in the range 3 T $< B_\perp <$ 12 T. In contrast, we observe a strong increase of the valley gap with increasing magnetic field [Fig. 3(b)] and find $\Delta E_V(\nu=3)=0.8$ meV. This is comparable to the results of magnetocapacitance studies by Khrapai *et al.*[2] on Si-MOS inversion layers who reported a valley energy gap of $\Delta E_V=0.5$ meV at $n_s=7.5\times10^{11}$ cm^{-2} and a strong dependence on magnetic field and filling factor. Pudalov *et al.*[36] reported a valley splitting of $\Delta E_V\,[\mathrm{meV}]\approx0.21+0.05B_\perp\,[\mathrm{T}]$ which yields 0.72 meV at $B_\perp=10.3$ T in agreement with our result at $\nu=3$.

The results obtained by magnetotransport measurements are ambiguous. Weitz *et al.*[7] determined the valley splitting from thermally activated transport in Si/SiGe. Taking into account the lower electron density in their sample the values obtained at $\nu=5,7,9$ agree well with our data. However, we do not observe the anomalous behavior found by these authors at $\nu=3$ which was attributed to an exchange-enhancement-induced level crossing of the upper valley branch of the lowest spin level and the lower valley branch of the upper spin level of the zeroth Landau level. Shlimak *et al.*[37] stated that there was no thermal activation process at odd filling factors in their Si/SiGe heterostructure of electron density similar to ours but with somewhat lower mobility and doubted the justification of the evaluation in Ref. 7. Koester *et al.*[6] investigated Si/SiGe heterostructures and found a valley splitting $\Delta E_V=52\ \mu$eV at $B_\perp=2.8$ T by means of SdH coincidence measurements. This value is similar to our result at $\nu=9$. However, the authors argued that the different shape of the confinement potential in Si/SiGe systems should lead to a significantly reduced valley splitting if compared to the values found for Si-MOS structures in earlier studies.[38] This is in contrast to our observation of a strong exchange enhancement at low odd filling factors, which is comparable to the results for Si-MOS inversion layers reported in Refs. 2 and 36.

The data presented in Fig. 9 for the $\nu=5$ energy gap provide clear evidence that the valley splitting does not depend on the total magnetic field B. Our finding supports the results of Weitz *et al.*[7] where the activation energy at valley filling factors was found to be independent of the tilt angle.

VII. CONCLUSIONS

We conclude that the de Haas–van Alphen effect studied on 2DES's in Si/SiGe in tilted magnetic fields provided a detailed insight into the energy-level structure and shape of the DOS. The energy splitting of the conduction-band valleys could be resolved in the dHvA effect in the high-field regime. The recalculated energy gap is $\sim$0.8 meV at $\nu=3$ without correcting for level broadening. One may speculate that a refined DOS model where the electron-electron interaction is taken into account in the presence of disorder might reveal an intrinsic value of ΔE_V which is even larger than 0.8 meV. For $\nu=5$ we showed that the dominant contribution to the valley splitting is independent of the tilt angle; i.e., it depends only on the perpendicular magnetic field. This is in contrast to the spin splitting which is also exchange driven but depends strongly on the total magnetic field B through the Zeeman energy. Here, the Coulomb exchange interaction leads to an enhanced spin gap. Evaluating the spin energy gap in tilted magnetic fields reveals a distinct dependence on $B_\parallel$ that differs from the dependence given by the Zeeman energy alone. The coincidence technique was successfully employed. This provided a new way in dHvA measurements to determine the size of the spin splitting that is complementary to the direct evaluation of the oscillation amplitudes. In particular, the coincidence technique yielded an energy gap that is not affected by the influence of disorder broadening and corresponded to a fixed $g^*_{co}=3.21$ for $\nu\geq10$. This behavior is in contrast to the common theoretical predictions, where g^* is found to be strongly dependent on the different spin-level occupancies.[26–28] However, this experimental finding is in excellent agreement with magnetotransport studies of samples from the same wafer.

ACKNOWLEDGMENTS

Financial support by the Deutsche Forschungsgemeinschaft via SFB 508 and Project No. Gr1640/1-3 in the "Schwerpunktprogramm Quanten-Hall Systeme" is gratefully acknowledged. The measurements at the HFML were financed by the Access to Research Infrastructures action of the European Union, Contract No. HPRI-CT-1999-00036.

*Electronic address: mwilde@physnet.uni-hamburg.de

[1] K. v. Klitzing, G. Dorda, and M. Pepper, Phys. Rev. Lett. **45**, 494 (1980).
[2] V. S. Khrapai, A. A. Shashkin, and V. T. Dolgopolov, Phys. Rev. B **67**, 113305 (2003).
[3] V. S. Khrapai, A. A. Shashkin, and V. T. Dolgopolov, Phys. Rev. Lett. **91**, 126404 (2003).
[4] K. Lai, W. Pan, D. C. Tsui, S. Lyon, M. Mühlberger, and F. Schäffler, Phys. Rev. Lett. **93**, 156805 (2004).
[5] D. Többen, F. Schäffler, A. Zrenner, and G. Abstreiter, Phys. Rev. B **46**, 4344 (1992).
[6] S. J. Koester, K. Ismail, and C. O. Chu, Semicond. Sci. Technol. **12**, 384 (1997).
[7] P. Weitz, R. J. Haug, K. von Klitzing, and F. Schäffler, Surf. Sci. **361**, 542 (1996).
[8] U. Zeitler, H. W. Schumacher, A. G. M. Jansen, and R. J. Haug, Phys. Rev. Lett. **86**, 866 (2001).
[9] K. Takashina, A. Fujiwara, S. Horiguchi, Y. Takahashi, and Y. Hirayama, Phys. Rev. B **69**, 161304(R) (2004).
[10] M. P. Schwarz, D. Grundler, I. Meinel, C. Heyn, and D. Heitmann, Appl. Phys. Lett. **76**, 3564 (2000).
[11] M. P. Schwarz, M. A. Wilde, S. Groth, D. Grundler, C. Heyn, and D. Heitmann, Phys. Rev. B **65**, 245315 (2002).
[12] F. Schäffler, Semicond. Sci. Technol. **12**, 1515 (1997).
[13] S. A. J. Wiegers, M. Specht, L. P. Lévy, M. Y. Simmons, D. A. Ritchie, A. Cavanna, B. Etienne, G. Martinez, and P. Wyder,

Phys. Rev. Lett. **79**, 3238 (1997).
[14] M. R. Schaapman, U. Zeitler, P. C. M. Christianen, J. C. Maan, D. Reuter, A. D. Wieck, D. Schuh, and M. Bichler, Phys. Rev. B **68**, 193308 (2003).
[15] J. P. Eisenstein, H. L. Stormer, V. Narayanamurti, A. Y. Cho, A. C. Gossard, and C. W. Tu, Phys. Rev. Lett. **55**, 875 (1985).
[16] A. Potts, R. Shepherd, W. G. Herrenden-Harker, M. Elliott, C. L. Jones, A. Usher, G. A. Jones, D. A. Ritchie, E. H. Linfield, and M. Grimshaw, J. Phys.: Condens. Matter **8**, 5189 (1996).
[17] J. G. E. Harris, R. Knobel, K. D. Maranowski, A. C. Gossard, N. Samarth, and D. D. Awschalom, Phys. Rev. Lett. **86**, 4644 (2001).
[18] M. Zhu, A. Usher, A. J. Matthews, A. Potts, M. Elliott, W. G. Herrenden-Harker, D. A. Ritchie, and M. Y. Simmons, Phys. Rev. B **67**, 155329 (2003).
[19] I. Meinel, D. Grundler, S. Bargstaedt-Franke, C. Heyn, D. Heitmann, and B. David, Appl. Phys. Lett. **70**, 3305 (1997).
[20] T. Ando, A. B. Fowler, and F. Stern, Rev. Mod. Phys. **54**, 437 (1982).
[21] F. J. Ohkawa and Y. Uemura, J. Phys. Soc. Jpn. **43**, 917 (1977).
[22] M. Wilde, Ph.D. thesis, Universität Hamburg, 2004.
[23] F. F. Fang and P. J. Stiles, Phys. Rev. **174**, 823 (1968).
[24] T. Englert, Solid State Commun. **40**, 893 (1981).
[25] R. J. Nicholas, R. J. Haug, K. v. Klitzing, and G. Weimann, Phys. Rev. B **37**, 1294 (1988).
[26] T. Ando and Y. Uemura, J. Phys. Soc. Jpn. **37**, 1044 (1974).
[27] A. H. MacDonald, H. C. A. Oji, and K. L. Liu, Phys. Rev. B **34**, 2681 (1986).
[28] A. Manolescu and R. R. Gerhardts, Phys. Rev. B **51**, 1703 (1995).
[29] H. W. Schumacher, A. Nauen, U. Zeitler, R. J. Haug, P. Weitz, A. G. M. Jansen, and F. Schäffler, Physica B **256–258**, 260 (1998).
[30] T. Ando and Y. Uemura, J. Phys. Soc. Jpn. **36**, 959 (1974).
[31] J. Luo, H. Munekata, F. F. Fang, and P. J. Stiles, Phys. Rev. B **41**, 7685 (1990).
[32] A. Schmeller, J. P. Eisenstein, L. N. Pfeiffer, and K. W. West, Phys. Rev. Lett. **75**, 4290 (1995).
[33] U. Zeitler, H. W. Schumacher, J. Regul, R. J. Haug, P. Weitz, A. G. M. Jansen, and F. Schäffler, Physica E (Amsterdam) **6**, 288 (2000).
[34] C. F. O. Graeff, M. S. Brandt, M. Stutzmann, M. Holzmann, G. Abstreiter, and F. Schäffler, Phys. Rev. B **59**, 13242 (1999).
[35] Z. Wilamowski, W. Jantsch, H. Malissa, and U. Rössler, Phys. Rev. B **66**, 195315 (2002).
[36] V. M. Pudalov, S. G. Semenchinskii, and V. S. Édel'man, JETP Lett. **41**, 325 (1985).
[37] I. Shlimak, V. Ginodman, M. Levin, M. Potemski, D. K. Maude, K.-J. Friedland, and D. J. Paul, Phys. Rev. B **68**, 075321 (2003).
[38] R. J. Nicholas, K. v. Klitzing, and T. Englert, Solid State Commun. **34**, 51 (1980).